Nanostructured Optical Fibre for use as Miniature Surface-enhanced Raman Scattering Sensors

A thesis submitted for the degree of

Doctor of Philosophy

by

Daniel Joshua White

Centre for Atom Optics and Ultrafast Spectroscopy

Faculty of Engineering and Industrial Sciences

Swinburne University of Technology

Melbourne, Australia

October 2, 2008

"No effect that requires more than ten percent accuracy in measurement is worth investigating."

— *Walther Nernst (1864-1941)*

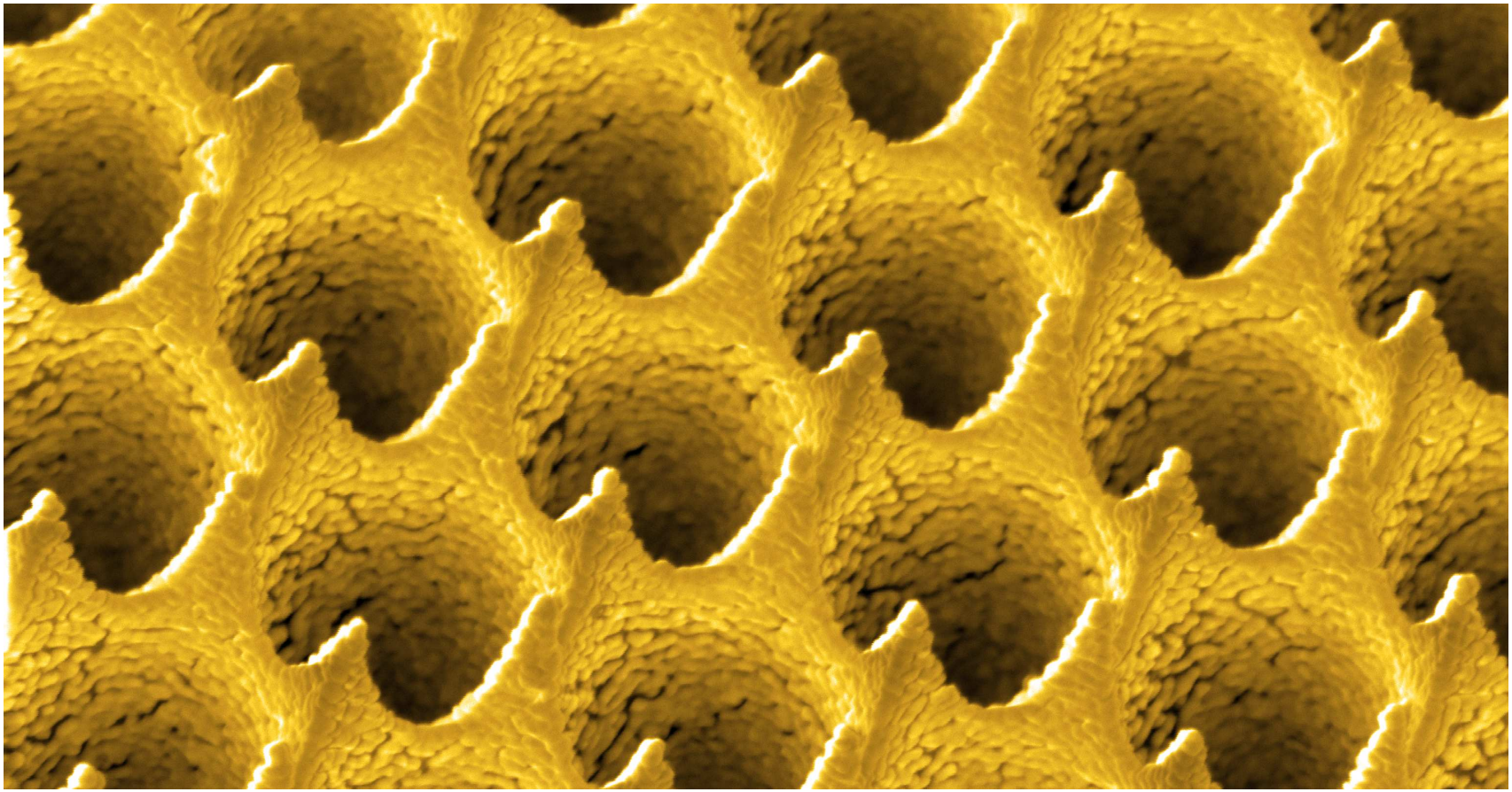

Fig. 1: False colour, high resolution SEM image of an etched nanostructured optical fibre with a metal coating. Field of view is approximately 1 μm $\times$ 2 μm.

Abstract

Surface-enhanced Raman scattering (SERS) is a powerful spectroscopic tool for detecting low concentrations of many substances. The SERS effect occurs when a Raman-active molecule interacts with the electromagnetic (EM) field generated by surface plasmon excitations in a metal surface having nanoscale structural features. As a result of the interaction, the typically weak Raman scattering is amplified by many orders of magnitude. Despite its usefulness, one of the factors that has so far prevented SERS from moving out of the laboratory and into the marketplace is a lack of affordable and reliable nanostructured substrates.

Since the discovery of the SERS effect over 30 years ago, many different techniques have been developed for producing the necessary substrate structures. Common techniques used include mechanical surface roughening, colloidal metal solutions, metal island films and lithographic techniques. While all produce SERS capable surfaces they either rely on random processes (which limit sample-to-sample reproducibility) or expensive manufacturing equipment. Both of these issues prevent cost effective commercialisation.

A novel alternative, which is investigated in this thesis, is to use an optical fibre based system. The fibres presented in this work are based on highly modified medical imaging fibres. These fibres consist of a fused bundle of single-mode fibres ("pixels") drawn in such a way that each fibre maintains its position along the length of the bundle. Previous works have shown that a selective chemical etchant can be used to erode the cores of these fibres leaving an array of wells. The work presented in this thesis shows that, by drawing the imaging fibre until the spacing between the cores is

of the order of hundreds of nanometres, the structures formed after etching are of a suitable scale for SERS. The glass itself is incapable of producing surface plasmons, so in order to generate the SERS functionality, the structures are coated with a thin layer of metal.

Initial fibre SERS sensors were produced by manually drawing commercially available imaging fibres to smaller diameters. As a result of the draw process, the initial inter-core spacing (the distance between two adjacent pixels) was reduced from approximately 4 μm to 150 - 650 nm. The cleaved tips of the fibres were then etched using a modified buffered hydrofluoric acid solution which resulted in the formation of nanostructures. The structures were then coated with silver and the fibre immersed in a solution of thiophenol for SERS testing. Due to difficulties in determining exactly how many molecules contributed to the SERS signal, an accurate measure of the SERS enhancement factor cannot be made. However, by estimating the molecular coverage density, an enhancement figure of $10^{5.3}$ to $10^{5.5}$ can be produced.

Although the manual drawing technique proved successful, lack of reproducibility meant that it was not suitable for large-scale commercial manufacturing. Before an attempt at manufacturing could be conducted, the parameters for the draw process (in particular temperature) needed to be determined. As the fibre is drawn by heating it to a high temperature in a furnace, it was necessary to understand the effects of the resultant diffusion of dopants within the fibre structure. To do this, a computer simulation was performed. The simulation package models a unit cell within the fibre structure and calculates firstly how the temperature affects the distribution of dopants and secondly, what the structures produced after etching would look like. It was found that in order to produce suitable nanostructures on the tips of the fibres, the diffusion length of the dopants must be less than 25% of the inter-core spacing. Knowing the maximum allowed diffusion length, means the maximum temperatures and heating times for manufacturing can be calculated.

After determining the desirable manufacturing conditions, a number of production attempts using commercial fibre drawing towers were made. Ultimately, a short length of suitable fibre was produced allowing a full characterisation of the SERS capabilities of the fibre to be conducted. It was found that despite the high reproducibility of the structures, for an optimised sensor, the SERS signal counts still varied by approximately 40% from sample to sample. Careful investigations of the surfaces indicated this variability is most likely due to the nature of the metal coating applied

rather than the fibre structures themselves. As such, it was found that to use sensors such as this for quantitative analysis, a form of internal SERS calibration is required. This was accomplished by exposing the sensor to a molecule of known concentration and measuring the signal intensity. After calibration, it was found the sample to sample variability dropped to approximately 8%.

As a practical demonstration of the use of the SERS fibres, experiments on the detection of glucose, CEES (a simulant for the nerve agent HD mustard) and chlorsulphuron (a commonly used herbicide), were conducted. To test the procedures for gathering quantitative results, the sensors used in the experiment were calibrated by applying a monolayer of 1-decanethiol. In addition to providing the calibration spectrum, this molecule also aids in bringing the target analytes close to the active surface. Characteristic spectral lines could be easily identified from solutions of 5,000 ppm glucose, 549 ppm CEES and 10,000 ppm chlorsulfuron. Results of these experiments also indicate that the SERS fibres are reversible, that is, capable of tracking both increasing and decreasing concentrations. While the sensitivity is, at this stage, low when compared to other substrate formats, the speed and ease with which measurements can be taken and the potential for further optimisation of the fibre's surface both indicate the significant potential of this technique.

Acknowledgements

This project started in 2004 with only my two supervisors and myself. Over the years though, the team grew and grew and as such, I have a fair few people to thank:

My family - parents Shirley and Alan, my sister Rebecca, my grandparents and my extended family. Without your encouragement and support throughout all my years of education, none of this would have been possible.

Dr. Paul Stoddart and Dr. Alex Mazzolini - my supervisors. Despite my previously limited experience in physics research, they took me in, taught me the ropes and supported me financially.

The folks in the Applied Optics research group - the successor to the Centre for Imaging and Applied Optics (CIAO) and now a part of the Centre for Atom Optics and Ultrafast Spectroscopy (CAOUS). Special thanks to Prof. Peter Cadusch for his help with all things mathematical. Thanks also to the other members: Jack, Annelene, Keith, Elena, Sasani and Felix for their support.

The crew at CAOUS: Prof. Peter Hannaford, centre leader and Tatiana Tchernova and Sharon Jesson, administrative staff. Thanks also to Dr. James Wang for assistance with the chromium coating. Extra thanks to Mark Kivinen, our workshop supervisor for building all those special items.

Mircea Petre and Sorin Theodorescu at OptoTech for the laser systems. Over the course of the project we were fortunate enough to be there during the development of the lasers and as such, enjoyed the ability to design systems to our exact specifications.

Hans Brinkies at the Industrial Research Institute of Swinburne (IRIS) for the polishing units and the Zeiss electron microscope.

Phil Francis and Yuxun Cao at the Royal Melbourne Institute of Technology (RMIT) for their help with the Philips electron microscope and the polishing units.

Finlay Shanks at Monash University for assistance with the Renishaw RM2000 Raman microscope.

Dr. Colin Cook at the Department of Primary Industries for his support on the chemistry side of the project and the use of the Renishaw InVia Raman microscope.

Dr. Katja Digweed, Dr. Justin Digweed, Ron Bailey, Peter Henry, Prof. John Canning and all the staff at the OFTC in the University of Sydney for their help during the nanostructured optical fibre manufacturing attempts.

Hiroki Sekiya and all the engineers and staff at Fujikura Asia Ltd for the imaging fibre modifications and the successful production of nanostructured optical fibres.

David Henderson, Tom Szafranski and the staff at Diamond Australia for their assistance in designing, manufacturing and polishing the ferrules.

Kaushal Vora at Minifab for his help with the initial hydrofluoric acid work.

Dr. Stuart Rumble at Lastek for his help in setting up the Raman microscopes and spectrometers.

Dr. Narelle Brack at La Trobe University for the use of the TOF-SIMS.

Last be certainly not least: to all my fellow students at the Swinburne Optics and Laser Laboratories during the years I was there. Far too many to mention you all but particular thanks go to Dave, Jack, Annelene, Michael, Peter, Linda, Tra My, Chris and Brendan who were around at the end when things got really stressful. Thanks to these guys, I found there's nothing that can't be fixed by stopping work and going to the pub! On that topic, thanks also to the crew at Mario's Coffee and Haddon's Bar for all those drinks.

Daniel White
Melbourne, Australia
October 2, 2008

Declaration

I, Daniel Joshua White, declare that this thesis entitled:

"Nanostructured Optical Fibre for use as Miniature Surface-enhanced Raman Scattering Sensors"

is my own work and has not been submitted previously, in whole or in part, in respect of any other academic award.

Daniel Joshua White

Centre for Atom Optics and Ultrafast Spectroscopy
Faculty of Engineering and Industrial Sciences
Swinburne University of Technology
Melbourne, Australia

Dated this day, October 2, 2008

Contents

Abstract **iii**

Acknowledgements **vi**

Declaration **ix**

Contents **x**

List of Figures **xv**

List of Tables **xx**

Glossary **xxi**

1 Project Motivation **1**

1.1 Vibrational Spectroscopy 1

1.2 Surface-enhanced Raman Spectroscopy 4

1.2.1 Enhancement Factors 6

1.3 Existing SERS Substrates 7

1.4 Optical Fibre Probes 10

1.4.1 Imaging Fibres 13

1.5 SERS Applications 14

1.6 Thesis Structure 15

2 Experimental Methods **17**

2.1 Introduction 17

2.2 Etching 17

2.2.1 Safety Procedures 19

2.3 Metal Film Deposition 20
2.3.1 SPI Module Sputter Coater 20
2.3.2 Kurt J. Lesker Sputter Coater 20
2.3.3 Emitech K950X Thermal Evaporation Coater 21

2.4 Electron Microscopy 22
2.4.1 Philips XL30 22
2.4.2 Zeiss Supra 40VP 22

2.5 Raman Systems 23
2.5.1 Renishaw RM2000 Raman Microscope 24
2.5.1.1 Laser Source 24
2.5.2 Horiba Jobin-Yvon Modular Raman Microscope 25
2.5.2.1 Laser Source 26
2.5.2.2 Triax 320 Spectrometer 27
2.5.3 Signal Acquisition 27

3 Prototype Nanostructured Optical Fibres 29

3.1 Introduction 29

3.2 Imaging Fibres 29
3.2.1 Structure 30

3.3 Fibre Etching 31
3.3.1 Fibre Preparation 32
3.3.2 Etching 33
3.3.3 Results and Analysis 34
3.3.3.1 Selectivity 34

3.4 SERS 36
3.4.1 Experimental Setup 36
3.4.2 Results and Analysis 38
3.4.3 Enhancement 39
3.4.3.1 Calculation 40

3.5 Dependence on Surface Features 42
3.5.1 Experimental Setup 44
3.5.2 Results and Analysis 50

3.5.2.1 Dependence on Inter-core Spacing 50
3.5.2.2 Dependence on Etch Time 50

3.6 Conclusions 51

4 Simulation of Etching Progression and Dopant Diffusion in Nanostructured Optical Fibres 53

4.1 Introduction 53

4.2 Computer simulation 54
4.2.1 Initial Conditions 54
4.2.2 Program Structure 56
4.2.3 Visualisation and Results 58

4.3 Diffusion 61
4.3.1 Theory 61
4.3.2 Analysis 62
4.3.3 Etch Rate Distribution with Diffusion 64
4.3.4 Results and Analysis 67

4.4 Conclusions 79

5 Production of Nanostructured Optical Fibre SERS Probes 81

5.1 Introduction 81

5.2 OFTC Fibre Production 82
5.2.1 First Design 82
5.2.2 Results 87
5.2.3 Second Design 88
5.2.4 Results 88
5.2.5 Analysis 89

5.3 Fujikura 91
5.3.1 Additional Manufacturing Attempts 93

5.4 Handling Methods 96
5.4.1 Mass Polishing 96
5.4.2 Ferrule Mounting 98

5.5 Conclusions 101

6 Characterisation of the Nanostructured Optical Fibre SERS Probe 103

6.1 Introduction 103

6.2 Etching Characterisation 103
6.2.1 Experimental Setup 103
6.2.2 Results and Analysis 104

6.3 SERS Characterisation 106
6.3.1 Experimental Setup 106
6.3.2 Results and Analysis 107

6.4 LSPR Characterisation 123
6.4.1 Experimental Setup 123
6.4.2 Results and Analysis 126

6.5 Repeatability Characterisation 127
6.5.1 Experimental Setup 127
6.5.2 Results and Analysis 128

6.6 Conclusions 130

7 Applications of the Nanostructured SERS Probe 133

7.1 Glucose Detection 134
7.1.1 Experiment and Results 135

7.2 CEES Detection 137
7.2.1 Experiment and Results 137

7.3 Chlorsulphuron Detection 139
7.3.1 Experiment and Results 140

7.4 Conclusions 142

8 Conclusions 144

8.1 Summary of the Project 144

8.2 Recommendations for Future Work 149

Bibliography 151

A Appendix A 161

B Appendix B **164**

Publications **178**

List of Figures

1 False colour, high resolution SEM image of an etched nanostructured optical fibre with a metal coating. ii

1.1 Vibrational processes. 2

1.2 The two forms of Raman scattering. 3

1.3 Schematic representation of the electromagnetic SERS process. 5

1.4 Metal coated mechanically roughened surfaces. 7

1.5 Colloidal metal structures. 8

1.6 Nanosphere based structures. 9

1.7 Metal coated lithographically prepared structures. 10

1.8 Multi-fibre and single-fibre Raman probes. 11

1.9 Imaging fibre components. 13

1.10 Chemically etched imaging fibre showing the wells formed in the locations of the pixel cores. 13

2.1 Renishaw RM2000 system. 24

2.2 HJY Modular Raman system schematic. 25

2.3 HJY Modular Raman system. 26

2.4 HJY Triax 320 spectrometer. 28

3.1 TOF-SIMS images of an FIGH-10-350S fibre 31

3.2 Drawn imaging fibre after etching using 10% HF for 15 & 30 minutes . 34

3.3 Drawn imaging fibre after etching using the BHF/HCl solution for 1, 2, & 10 minutes . . . 35

3.4 Thiophenol molecule. . . . 37

3.5 SERS signals of thiophenol from fibres etched for 1 & 2 minutes. . . . 38

3.6 NRS spectrum of bulk thiophenol . . . 39

3.7 Structure dependence on fibre size given a fixed etch duration . . . 43

3.8 Fibres with an inter-core spacings of 250, 420 & 650 nm after 30 seconds etching using BHF solution. . . . 45

3.9 Structure dependence on etch duration. . . . 46

3.10 Raman intensity vs. inter-core spacing. . . . 48

3.11 Raman intensity vs. etch duration. . . . 49

4.1 Rectangular unit cell and simulation region in a hexagonal lattice. . . . 54

4.2 Initial etch rate distribution. . . . 55

4.3 Quantised particle exposure. . . . 57

4.4 Particle exposures curve. . . . 57

4.5 Simulation output for fibre based on initial conditions. . . . 59

4.6 Simulation output for fibre based on initial conditions at 27, 28 and 29 seconds. . . . 60

4.7 Diffusion coefficient and D_L as a function of temperature and time. . . 63

4.8 Diffusion lengths at 1000, 1250, 1500 & 1750°K. . . . 64

4.9 Time / temperature curves for various D_L. . . . 65

4.10 Convolution template and corresponding unit cell etch rate distributions for D_L of 20, 100 & 180 nm. . . . 66

4.11 Illustrated cross section of simulation data showing definitions of well depth and pyramid height. . . . 67

4.12 Simulation output for various ξ_d ratios after a simulation etch time of 10 s. . . . 68

4.13 Simulation output for various ξ_d ratios after a simulation etch time of 20 s 69

4.14 Simulation output for various ξ_d ratios after a simulation etch time of 30 s. 70

4.15 Simulated pyramids heights of various ξ_d for a fibre with $I_C = 400$ nm. 71

4.16 Second differential of the pyramid heights. 72

4.17 Simulated well depths of various ξ_d. 73

4.18 Second differential of the well depths. 74

4.19 Wall break-through and pyramid equilibrium times for various ξ_d. . . . 76

4.20 Faceting to find the surface area. 77

4.21 Estimated unit cell surface area for ξ_d from 15% to 45%. 77

4.22 Cross-section of a simulated well for a fibre with $\xi_d = 25\%$ showing the pyramid height and well depth equilibriums. 78

4.23 Temperature / time graph for ξ_d of 25%. 80

5.1 OFTC fibre production tower. 84

5.2 Schematic of the OFTC fibre production tower. 85

5.3 OFTC drawn imaging fibre (design 1) after etching using BHF solution. 87

5.4 OFTC fibre with a diameter of 110 μm 89

5.5 D_L for the temperatures encountered during the draw attempts. 90

5.6 Etched FIGH-30-100X fibre and simulated fibre with diffusion. 92

5.7 Temperature versus time graph for $\xi_d = 20\%$. 93

5.8 FIGH-30-400X fibre. 94

5.9 Block mounted fibres. 96

5.10 SEM images of block mounted fibres showing surface damage after first polishing attempt. 97

5.11 SEM images of block mounted fibres showing surface damage after second polishing attempt. 98

5.12 Diamond FO ferrule design. 99

5.13 Fibre mounted inside ferrule. 100

5.14 Scratched ferrule mounted fibre after etching. 101

6.1 Etched FIGH-30-100X after 1 - 20 minutes etching. 105

6.2 Etched fibre with 20.4 nm silver coating. 107

6.3 Etched fibre with 40.5 nm silver coating. 108

6.4 Etched fibre with 60.2 nm silver coating. 108

6.5 Etched fibre with 80.5 nm silver coating. 109

6.6 Etched fibre with 100.0 nm silver coating. 109

6.7 Example SERS spectrum. 111

6.8 Average thiophenol peak intensity ($\overline{I_{tp}}$) for samples coated with 20.5 nm silver. 112

6.9 Average thiophenol peak intensity for samples coated with 40.5 nm silver. 113

6.10 Average thiophenol peak intensity for samples coated with 60.2 nm silver. 114

6.11 Average thiophenol peak intensity for samples coated with 80.5 nm silver. 115

6.12 Average thiophenol peak intensity ($\overline{I_{tp}}$) for samples coated with 100.0 nm silver. 116

6.13 SERS signal counts for all samples. 117

6.14 Contour plot of $\overline{I_{tp}}$. 118

6.15 Surface plot of $\overline{I_{tp}}$. 119

6.16 Silver particles on the walls of the wells. 122

6.17 Micro-spectrophotometer schematic. 124

6.18 Micro-spectrophotometer. 124

6.19 Localised surface plasmon resonances. 125

6.20 NRS spectrum of silicon. 128

6.21 Spectra for repeatability study. 129

6.22 Spectra for the repeatability study after normalising to the 1073 cm^{-1} peak. 131

7.1 1-decanethiol molecule. 134

7.2 $\alpha-$D glucose molecule. 135

7.3 1-decanethiol and $\alpha-$D glucose spectra with the characteristic glucose peaks identified. 136

7.4 CEES molecule. 137

7.5 1-decanethiol and CEES spectra with the characteristic CEES peaks identified. 138

7.6 Chlorsulphuron molecule. 139

7.7 1-decanethiol and 10,000ppm chlorsulphuron spectra with the characteristic chlorsulphuron peaks identified. 140

7.8 Chlorsulphuron reversibility. 141

B.1 Simulation output for fibre with no diffusion. 168

B.2 Simulation output for fibre with $\xi_d = 5\%$. 169

B.3 Simulation output for fibre with $\xi_d = 10\%$. 170

B.4 Simulation output for fibre with $\xi_d = 15\%$. 171

B.5 Simulation output for fibre with $\xi_d = 20\%$. 172

B.6 Simulation output for fibre with $\xi_d = 25\%$. 173

B.7 Simulation output for fibre with $\xi_d = 30\%$. 174

B.8 Simulation output for fibre with $\xi_d = 35\%$. 175

B.9 Simulation output for fibre with $\xi_d = 40\%$. 176

B.10 Simulation output for fibre with $\xi_d = 45\%$. 177

List of Tables

3.1 Variables for signal intensity enhancement calculation. 40
3.2 Signal intensity enhancements. 40

4.1 Diffusion parameters for a germanium doped fibre. 62
4.2 Wall break-through, pyramid equilibrium and well depth equilibrium times for a fibre with $I_C = 400$ nm. 75
4.3 Equilibrium pyramid heights, well depths and estimated unit cell surface areas for a fibre with $I_C = 400$ nm. 78

5.1 MCVD parameters for the first design. 83
5.2 Fibre size regimes for the first design. 83
5.3 Draw parameters for the first design. 86
5.4 Draw parameters for design 2. 88
5.5 D_L and ξ_d ratios for both designs taking into account estimated temperatures and times inside the furnace. 90
5.6 Summary of nanostructured optical fibre industrial scale manufacturing attempts. 95

A.1 Values used for SERS enhancement calculation. 161

Glossary

AFM	Atomic Force Microscope
BHF	Buffered Hydrofluoric Acid
CCD	Charge Coupled Device
CEES	2-chloroethyl ethyl sulfide
cps/mW	Counts-per-second per milliwatt
D_L	Diffusion length
E	SERS Enhancement Factor
EM	Electromagnetic
EFL	Effective Focal Length
FON	Film-on-Nanosphere
GCMS	Gas Chromatography - Mass Spectroscopy
HCl	Hydrochloric Acid
HDPE	High Density Polyethylene
HF	Hydrofluoric Acid
HJY	Horiba Jobin-Yvon Modular Raman Microscope
FWHM	Full-width half-max
I_C	Inter-core spacing
$\overline{I_{tp}}$	Average intensity of thiophenol peaks
KJL	Kurt J. Lesker Coating Unit
LCMS	Liquid Chromatography - Mass Spectroscopy
LSPR	Localised Surface Plasmon Resonance
MCVD	Modified Chemical Vapor Deposition
n	Refractive Index
N.A.	Numerical Aperture
NRS	Normal Raman Spectroscopy
NSL	Nanosphere Lithography
OFTC	Optical Fibre Technology Centre

PP	Polypropylene
ppm	Parts-per-million
SAM	Self-assembled Monolayer
SEM	Scanning Electron Microscope
SERS	Surface Enhanced Raman Spectroscopy
TEC	Thermo-electric Cooler
TOF-SIMS	Time-of-flight Secondary Ion Mass Spectrometer
ξ_d	Smearing ratio (D_L to I_C ratio)